Quantitative Description of Spatially Homogeneous Textures by Characteristic Grey Level Co-Occurrences *

Georgy Gimel'farb

Centre for Image Technology and Robotics
Department of Computer Science, Tamaki Campus
University of Auckland, Auckland, New Zealand

Abstract

Gibbs random field model with multiple pairwise pixel interactions describes each type of spatially homogeneous image textures in terms of a pixel neighbourhood and Gibbs potentials that specify the geometric structure and quantitative strengths of interactions, respectively. Each image is represented by a set of grey level co-occurrence histograms which are sufficient statistics of the model. The histograms permit us to analytically approximate Gibbs potentials and recover most characteristic neighbourhood from a given training sample so that the model provides a theoretical framework for texture description by intergal histogram-based features.

Keywords: **texture, Gibbs random field, grey level co-occurrence, interaction structure.**

1. Introduction

We restrict our consideration to the simplest notion of spatial homogeneity of image textures: they are assumed to be homogeneous if conditional probability distributions of grey levels are translation–invariant. Generally, the probability distribution of grey levels in a pixel depends only on grey levels in a characteristic pixel neighbourhood, i.e. a subset of pixels with fixed relative displacements from the pixel. This translation–invariant neighbourhood specifies the geometric structure of interactions. Each interacting pixel pair is the second-order clique of the neighbourhood graph connecting all the interacting pixels [2], and image-wide translation–invariant pairwise pixel interactions are stratified into several clique families, consisting each of translation invariant cliques with a particular inter–pixel displacement. For the Gibbs random field model with multiple pairwise interactions [3, 4], each clique family has its Gibbs potential that relates the quantitative strength of pixel interactions to grey level co-occurrences (GLC) in a clique.

The sum of the potential values over a clique family, called the partial interaction energy, determines the contribution of the family to the entire Gibbs probability of a particular image. The partial energy depends only on the Gibbs potential and the GLC histogram (GLCH) collected for the clique family so that the GLCHs are the sufficient statistics of this Gibbs model [3, 4]. Given the interaction structure and potentials, the images with the same GLCHs are equiprobable and hence nondistinct with respect to the model. Therefore, each type of spatially homogeneous image textures is completely described by a subset of GLCHs specified by the characteristic pixel neighbourhood.

Different integral GLCH-based texture features have been used in image analysis over many years [7, 6] but with an entirely heuristic choice of the pixel neighbourhood to collect the histograms. In what follows we overview in brief the parameter estimation for the models with multiple pairwise interactions [3, 4]. Our goal is to show that a complete quantitative description of two specific types of spatially homogeneous images, namely, stochastic and regular textures, should be based on the characteristic pixel neighbourhood. Experiments in simulating textures from [1] show that such description is representative of basic visual features of the textures.

2. Basic definitions and notation

Let $\mathbf{R} = \{(x, y) : \; x = \overline{0, M-1};\; y = \overline{0, N-1}\}$ be a finite $M \times N$ arithmetic lattice. For brevity, we denote $\mathbf{i} = (x, y)$ the lattice sites. Let $\mathbf{g} = [g_{\mathbf{i}} : \mathbf{i} \in \mathbf{R};\; g_{\mathbf{i}} \in \mathbf{Q}]$ be a digital image with a finite set $\mathbf{Q}$ of grey levels.

An interaction structure in $\mathbf{R}$ is presented by a subset of clique families $\mathbf{C} = \{\mathbf{C}_a : \; a \in \mathbf{A}\}$ where $\mathbf{A}$ is a set of indices. Each family $\mathbf{C}_a = \{(\mathbf{i}, \mathbf{j}) : \; \mathbf{i}, \mathbf{j} \in \mathbf{R};\; \mathbf{i} - \mathbf{j} = \mathbf{n}_a\}$ consists of translation invariant cliques $(\mathbf{i}, \mathbf{j})$ with a fixed relative displacement $\mathbf{n}_a = (\delta x_a, \delta y_a)$ between the pixels $\mathbf{i}$ and $\mathbf{j}$. The pixel neighbourhood $\mathbf{N_A} = \{\mathbf{n}_a : \; a \in \mathbf{A}\}$ that specifies the structure $\mathbf{C}$ is a subset of a large search set $\mathbf{W}$ of all the neighbours with the bounded inter-pixel displacements $\mathbf{W} = \{(\delta x, \delta y) : \; |\delta x| \le \delta x_{\max};\; |\delta y| \le \delta y_{\max}\}$.

Let $\mathbf{V}_a$ be a Gibbs potential for the clique family $\mathbf{C}_a$. The potential values depend on the GLCs $(q = g_{\mathbf{i}}, s = g_{\mathbf{j}}) \in \mathbf{C}_a$:

$$\mathbf{V}_a = \left[\, V_a(q, s) \;\; : \;\; (q, s) \in \mathbf{Q}^2 \,\right].$$

*This work was supported in part by the University of Auckland Research Committee grant XXXXX/9343/3414083.

Each clique family influences the Gibbs probability of an image $\mathbf{g}$ via the partial interaction energy

$$\begin{aligned} E_a(\mathbf{g}) &= \sum_{(\mathbf{i},\mathbf{j})\in\mathbf{C}_a} V_a(g_\mathbf{i}, g_\mathbf{j}) \\ &= \sum_{(q,s)\in\mathbf{Q}^2} V_a(q,s) H_a(q,s|\mathbf{g}) \\ &\equiv \mathbf{V}_a \bullet \mathbf{H}_a(\mathbf{g}) = |\mathbf{C}_a| \cdot \mathbf{V}_a \bullet \mathbf{F}_a(\mathbf{g}) \end{aligned} \quad (1)$$

where $\bullet$ denotes the dot product, $|\ldots|$ is the set cardinality, $\mathbf{H}_a(\mathbf{g})$ is the GLCH for the family $\mathbf{C}_a$ collected over the image $\mathbf{g}$:

$$\mathbf{H}_a(\mathbf{g}) = \left[\, H_a(q,s|\mathbf{g}) \ : \ (q,s) \in \mathbf{Q}^2 \,\right],$$

and $\mathbf{F}_a$ denote the normalised GLCH, or the relative sample frequency distribution of GLCs:

$$\begin{aligned} \mathbf{F}_a(\mathbf{g}) &= \frac{1}{|\mathbf{C}_a|}\, \mathbf{H}_a(\mathbf{g}) \\ &\equiv \left[F_a(q,s|\mathbf{g}) = \frac{H_a(q,s|\mathbf{g})}{|\mathbf{C}_a|} \ : \ (q,s) \in \mathbf{Q}^2 \right]. \end{aligned}$$

The GLCH-based Gibbs image model with multiple pairwise pixel interactions [3, 4] is specified by the neighbourhood $\mathbf{N_A}$ and potential $\mathbf{V}$, and relates the Gibbs probability of a sample $\mathbf{g}$:

$$\Pr(\mathbf{g}|\mathbf{N_A}, \mathbf{V}) = \frac{1}{Z_{\mathbf{N_A},\mathbf{V}}} \exp\left(E(\mathbf{g})\right) \quad (2)$$

to the total interaction energy of the sample:

$$\begin{aligned} E(\mathbf{g}) = \sum_{a\in\mathbf{A}} E_a(\mathbf{g}) &= \mathbf{V} \bullet \mathbf{H}(\mathbf{g}) \\ &= |\mathbf{R}| \cdot \mathbf{V} \bullet \mathbf{F}(\mathbf{g}). \end{aligned} \quad (3)$$

Here, $\mathbf{V} = [\mathbf{V}_a \ : \ a \in \mathbf{A}]$, $\mathbf{H}(\mathbf{g}) = [\mathbf{H}_a(\mathbf{g}) \ : \ a \in \mathbf{A}]$, and $\mathbf{F}(\mathbf{g}) = [\rho_a \mathbf{F}_a(\mathbf{g}) \ : \ a \in \mathbf{A}]$ denote the entire potential vector, the entire GLCH vector, and the entire weighted normalised GLCH vector, respectively, for the interaction structure specified by the characteristic neighbourhood $\mathbf{N_A}$. The weight $\rho_a = \frac{|\mathbf{C}_a|}{|\mathbf{R}|}$, relating the cardinality of the clique family to the lattice cardinality, tends to unity when the lattice size increases.

3. Potential estimation

The maximum likelihood estimate (MLE) of the potential $\mathbf{V}$ has the simple first approximation [3, 4]:

$$\widetilde{\mathbf{V}} = \lambda_0 \left[\rho_a \Delta_{a,0}(\mathbf{g}^\circ) \ : \ a \in \mathbf{A}\right] \quad (4)$$

where $\Delta_{a,0}(\mathbf{g}^\circ) = \mathbf{F}_a(\mathbf{g}^\circ) - \mathbf{F}_{\mathrm{irf}}$ denotes the difference between the normalised GLCH $\mathbf{F}(\mathbf{g}^\circ)$ for a given training sample $\mathbf{g}^\circ$ and the like expected histogram, i.e. the marginal probability distribution of GLCs

$$\mathbf{F}_{\mathrm{irf}} = \left[\frac{1}{|\mathbf{Q}|^2} \ : (q,s) \in \mathbf{Q}^2 \right]$$

for the independent random field (IRF). The IRF is described by the model of Eq. (2) with zero potential $\mathbf{V} = \mathbf{0}$. The scaling factor λ_0 in Eq. (4) is almost independent of the normalised GLCHs:

$$\lambda_0 = \frac{\sum_{a\in\mathbf{A}} \rho_a^2 \sum_{(q,s)\in\mathbf{Q}^2} \Delta_{a,0}^2(q,s|\mathbf{g}^\circ)}{\phi_{\mathrm{glc}} \sum_{a\in\mathbf{A}} \rho_a^3 \sum_{(q,s)\in\mathbf{Q}^2} \Delta_{a,0}^2(q,s|\mathbf{g}^\circ)} \approx \frac{1}{\phi_{\mathrm{glc}}} \quad (5)$$

where

$$\phi_{\mathrm{glc}} = \frac{1}{|\mathbf{Q}|^2} \left(1 - \frac{1}{|\mathbf{Q}|^2}\right) \approx \frac{1}{|\mathbf{Q}|^2}$$

is the variance of the relative sample frequencies for the IRF. When the lattice size $|\mathbf{R}|$ increases, the ratios ρ_a tend to unity so that the potential estimate in Eqs. (4) and (5) is practically independent of the lattice size.

Under an additional natural constraint that the sample $\mathbf{g}^\circ$ should keep the least upper bound of the rank in the total Gibbs energy among all the images, the analytic form of Eq. (4) holds also for the potentials themselves [4]:

$$\mathbf{V} = \left[\lambda_a \Delta_{a,0}(\mathbf{g}^\circ) \ : \ a \in \mathbf{A}\right], \quad (6)$$

and only the factors $\Lambda = [\lambda_a \ : \ a \in \mathbf{A}]$ have to be estimated for finding the potential MLE.

4. Characteristic neighbourhood

The higher the difference $\Delta_{a,0}(\mathbf{g}^\circ)$, the greater the impact of the clique family $\mathbf{C}_a$ on the Gibbs probability of the training sample $\mathbf{g}^\circ$. Therefore a characteristic pixel neighbourhood that specifies the interaction structure can also be estimated from the GLCHs for a large search set $\mathbf{W}$ of clique families by using the partial energies of Eq. (1) or other integral measures, e.g. the chi-square distances between the GLCHs.

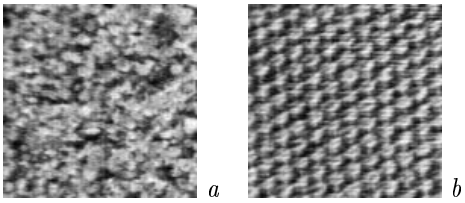

Figure 1: Stochastic textures D29 "Beach sand" (a) and D77 "Cotton canvas" (b) from [1].

Because all clique families share the same pixels, the GLCHs are not statistically independent, and to find a characteristic neighbourhood one has to know how strong are their dependences. The simplest assumption in [3, 4] that all clique families are (almost) independent defines a class of stochastic textures. Two examples of such textures are shown in Figure 1. In this case the characteristic neighbourhood can be found by choosing the clique families with the partial energies over a particular threshold. The threshold is derived from the relative frequency distribution of these energies over the search set $\mathbf{W}$.

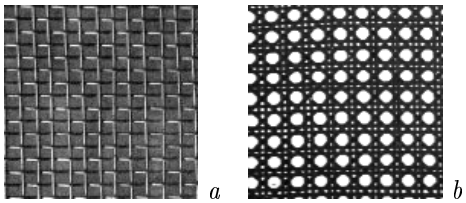

Figure 2: Regular textures D1 "Woven wire" (a) and D101 "Cane" (b) from [1].

The above assumption does not hold for regular textures such as shown in Figure 2. These textures have the determining (basic) and minor (fine) repetitive details, and both types are visually important. But the partial energies for independent clique families governing a fine interaction structure are usually lower than the threshold computed under the assumption that all the interactions are independent. A simple model of dependences between the GLCHs separates the interactions in the search set $\mathbf{W}$ into two categories: primary interactions and secondary interactions. Only the primary interactions are assumed to be (almost) statistically independent and hence characteristic for describing a texture. The secondary interactions are produced by a statistical interplay of the primary ones and need not be included to a characteristic neighbourhood. This more general assumption permits us to sequentially estimate a neighbourhood that consists only of the primary interactions and describes both the basic and fine repetitive details.

4.1. Parallel neighbourhood estimation

Under the simplest assumption that all the interactions are (almost) independent, the characteristic interaction structure of a stochastic texture is recovered by comparing the partial Gibbs energies to the threshold $\theta = E_{\mathrm{m}} + k\sigma$ depending on their relative sample frequency distribution for the search set $\mathbf{W}$. Here, E_{m} and σ are the mean energy and standard deviation, respectively. In our experiments the factor k is mostly chosen in the range $3 \leq k \leq 5$.

Because the scaling factor λ_0 is the same for all the clique families, the basic structure is recovered using the relative partial energies

$$e_a(\mathbf{g}^\circ) = \rho_a \mathbf{F}_a(\mathbf{g}^\circ)\Delta_{a,0}(\mathbf{g}^\circ); \qquad a \in \mathbf{W}, \tag{7}$$

for the training sample. The relative partial energy is Practically the same basic structures are recovered by thresholding the chi-square distances $\chi^2_a(\mathbf{F}_a(\mathbf{g}^\circ), \mathbf{F}_{\mathrm{irf}})$ between the normalised GLCHs for the training sample and the marginal probability distribution for the IRF.

4.2. Sequential neighbourhood estimation

Let $\mathbf{C}_\alpha$ and $\mathbf{C}_\beta$ be the independent clique families with significant partial energies for the training sample $\mathbf{g}^\circ$. Then their statistical interplay produces the dependent families $\mathbf{C}_\gamma$, such that $\mathbf{n}_\gamma = 2 \cdot \mathbf{n}_\alpha$, or $\mathbf{n}_\gamma = 2 \cdot \mathbf{n}_\beta$, or $\mathbf{n}_\gamma = \mathbf{n}_\alpha + \mathbf{n}_\beta$, and so forth, that can possess also a significant although somewhat lower energy. In other words, if the normalised GLCHs $\mathbf{F}_\alpha(\mathbf{g}^\circ)$ and $\mathbf{F}_\beta(\mathbf{g}^\circ)$ differ much from the marginal distribution $\mathbf{F}_{\mathrm{irf}}$ for the IRF, the similar difference for the GLCH $\mathbf{F}_\gamma(\mathbf{g}^\circ)$ can also be quite large.

Assuming that all the interactions are subdivided into the independent primary and dependent secondary interactions, a characteristic neighbourhood is reduced in size and the fine interaction structure is recovered by iteratively eliminating the secondary interactions [8, 5]. At every iteration t, a clique family which is most characteristic with respect to the previously found interaction structure is selected and added to this structure.

4.2.1. Empirical scheme

The empirical estimation in [8] performs at every iteration t the followimg two successive steps.

1. (*Texture simulation*) A new texture sample $\mathbf{g}_{[t]}$ is simulated under a current interaction structure $\mathbf{C}_{[t]} = \{\mathbf{C}_a : a \in \mathbf{A}_{[t]}\}$.
2. (*Selection of a clique family*) The normalised training GLCHs $\{\mathbf{F}_a(\mathbf{g}^\circ) : a \in \mathbf{W}\}$ are compared to the GLCHs $\{\mathbf{F}_a(\mathbf{g}_{[t]}) : a \in \mathbf{W}\}$ for the simulated sample $\mathbf{g}_{[t]}$ to select the most characteristic primary clique family and add it to the current structure.

The selection can be based on the maximum relative partial energy

$$e_a(\mathbf{g}^\circ) = \rho_a \cdot \mathbf{F}_a(\mathbf{g}^\circ) \bullet \big(\mathbf{F}_a(\mathbf{g}^\circ) - \mathbf{F}_a(\mathbf{g}_{[t]})\big) \tag{8}$$

but better results are obtained by using the chi-square distance $\chi^2_a(\mathbf{F}_a(\mathbf{g}^\circ), \mathbf{F}_a(\mathbf{g}_{[t]})$ between the GLCHs.

In principle, the simulation step takes account of all the dependences between the interactions so that the structure of the minimum size is expected to be found. But the empirical scheme has at least two drawbacks. First, it involves a large body of computations for simulating the samples as the time for generating each sample is proportional to the current size $|\mathbf{A}_t|$ of the neighbourhood. Thus the total time is quadratic with respect to the final neighbourhood size. Secondly, the simulation produces a variety of different samples $\mathbf{g}_{[t]}$ with the GLCHs $\mathbf{F}_a(\mathbf{g}_{[t]})$ that approach the training GLCHs only on the average. Therefore the selected clique families reflect also a particular sequence of simulated images so that the same training sample gives rise to different characteristic neighbourhoods, especially, as concerning the fine structure.

4.2.2. Approximate analytical scheme

Assuming that the primary GLCHs are statistically independent, the GLCHs for the secondary interactions can be analytically approximated by recomputing each current non-primary GLCH, $\mathbf{F}_\gamma(\mathbf{g})$, using the last chosen primary GLCH, $\mathbf{F}_\alpha(\mathbf{g})$, and the previous GLCH,

$\mathbf{F}_\beta(\mathbf{g})$, such that $\mathbf{n}_\gamma = \mathbf{n}_\alpha + \mathbf{n}_\beta$. In this case the GLCHs in the search set $\mathbf{W}$ are analytically updated after adding each next primary clique family to the current interaction structure [5].

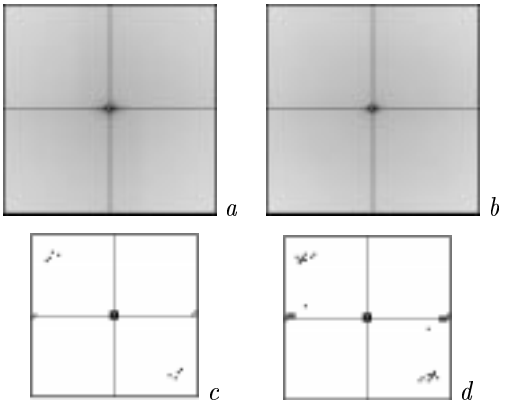

Figure 3: Texture D29: the computed (a) and actual (b) Gibbs energies for the Gibbs model in Eq. (2) with the 10 analytically chosen clique families and the analytically chosen neighbourhoods of the 10 (c) and 22 (d) clique families with the top relative energy.

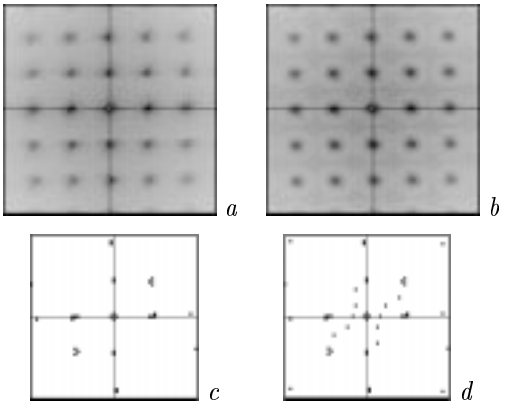

Figure 4: Texture D101: computed (a) and actual (b) Gibbs energies for the Gibbs model in Eq. (2) with the 15 analytically chosen clique families and the analytically chosen neighbourhoods of the 15 (c) and 22 (d) clique families with the top relative energy.

Figures 3, *a*-*b*, and 4, *a*-*b*, demonstrate the grey-coded actual and analytically computed distributions of the relative partial energies of Eq. (7) for the textures D29 and D101 over the search set $\mathbf{W}$. This latter set is displayed as the 325×325 window, each square box 4×4 representing a particular inter-pixel displacement $(\delta x, \delta y)$; $-40 \leq \delta x, \delta y \leq 40$. The secondary GLCHs are recomputed from the centre to the borders of the window $\mathbf{W}$ to roughly approximate the main part of the statistical interplay between the primary interactions. The corresponding interaction structures as well as the more detailed structures with the 22 clique families are shown in Figures 3, *c*-*d*, and 4, *c*-*d*.

In these examples the reduced basic structure of the texture D29 contains the two highly energetic clique families with the inter-pixel displacements $\{(1,0),(0,1)\}$. All other families are two or more orders of magnitude lower in the relative energies. As a result, the chosen fine structure of this texture contains only non-characteristic long-range interactions that do not represent specific visual features and are obviously arbitrary, as distinct from the characteristic fine structure of the regular texture D101. As will be shown later, the sequential search for the top relative chi-square distances results in more efficient neighbourhoods for the stochastic texture D29.

The analytical scheme gives a reasonable fit to the actual partial energies as well as to the GLCHs for the clique families. Therefore it is of interest to experimentally compare this scheme to the empirical one.

5. Texture simulation experiments

We generate textures by the controllable simulated annealing (CSA) introduced in [3, 4]. The CSA exploits the Gibbs model in Eq. (2) with the fixed characteristic pixel neighbourhood $\mathbf{N_A}$ to produce a nonstationary Markovian chain of images. Each successive image, $\mathbf{g}_{[t]}$, $t = 1, 2, \ldots, T$, is obtained from the preceding one, $\mathbf{g}_{[t-1]}$, by stochastic relaxation using the Metropolis sampler [2] with a concurrent adaptation of the potential, $\mathbf{V}_{[t]}$. Each macrostep t traces randomly without repetition the entire lattice $\mathbf{R}$. The potential adaptation provides for stochastic approximation of the training GLCHs $\{\mathbf{F}_a(\mathbf{g}^\circ) : a \in \mathbf{A}\}$ with the GLCHs for the generated images.

Below, each individual simulation experiment uses $T = 300$ macrosteps of the CSA with the same control parameters that have been used in [4] to generate different stochastic textures. All the training and simulated samples are of size 128×128 pixels, unless otherwise specified, and the search set $\mathbf{W}$ represents 3280 clique families within the bounds $\delta x_{\max} = 40, \delta y_{\max} = 40$.

5.1. Simulation with the neighbourhoods estimated in parallel

Figures 5 – 8 show the CSA-simulated samples of the textures D1, D29, D77, and D101 from [1]. The training samples were shown in Figures 1 and 2. Characteristic neighbourhoods of different size, estimated in parallel for the stochastic textures D29 and D77, result in a good visual quality of simulation. Here, the neighbourhoods selected by thresholding the partial Gibbs energies or chi-square distances from the IRF are almost the same.

At the same time the estimated structures of the regular textures D1 and D101 reproduce only roughly the repetitive fine details of the original patterns, and the larger sizes of the neighbourhoods do not significantly improve the simulation.

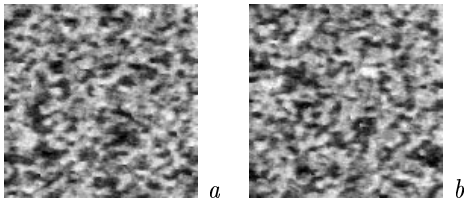

Figure 5: Texture D29: CSA-simulation with the neighbourhoods of 11 clique families found by thresholding the chi-square distances (a) and the partial Gibbs energies (b).

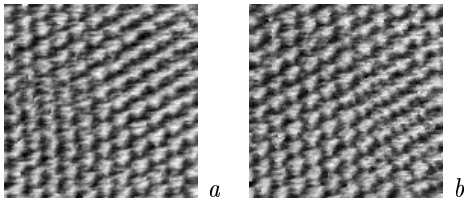

Figure 6: Texture D77: CSA-simulation with the neighbourhoods of 44 (a) and 125 (b) clique families found by thresholding the chi-square distances.

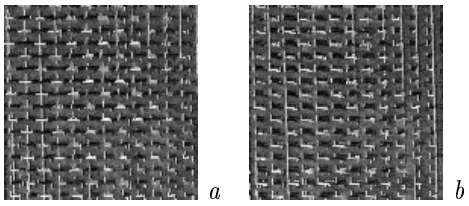

Figure 7: Texture D1: CSA-simulation with the basic structures of 48 (a) and 73 (b) clique families found by thresholding the chi-square distances.

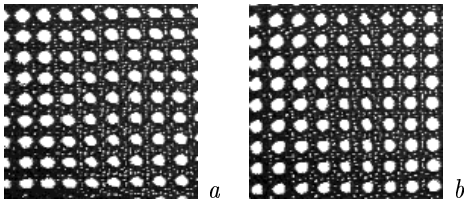

Figure 8: Texture D101: CSA-simulation with the neighbourhoods of 39 (a) and 63 (b) clique families learned by thresholding the partial Gibbs energies.

5.2. Simulation with the neighbourhoods estimated sequentially

Figure 9 shows the samples of the texture D29 simulated with the characteristic neighbourhoods found for the training sample in Figure 1, *a*, by the energy-based empirical sequential choice. As indicated earlier (see Figure 3), the actual energy distribution over $\mathbf{W}$ is closely approximated by the statistical interplay of only the two clique families with inter-pixel displacements $(1,0)$ and $(0,1)$. Another clique families are chosen rather arbitrary among the remaining families with very low relative Gibbs energies, and the final interaction structure is unsuitable for simulating the texture samples that are visually similar to the training sample. The images in Figure 9, in contrast to the simulated samples in Figure 5, differ much from the training sample even when the overall interaction structure has the greater size than the structure found by thresholding the partial energies.

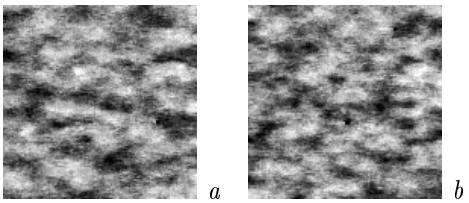

Figure 9: Texture D29: CSA-simulation with the 7 (a) and 11 (b) clique families found by the sequential empirical choice of the top relative partial energy.

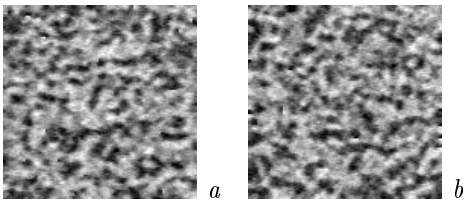

Figure 10: Texture D29: simulation with the 8 (a) and 12 (b) clique families found by the sequential empirical choice of the top relative chi-distance.

At the same time, the empirical sequential choice of the top chi-square distance produces much better neighbourhoods for this texture. The simulated samples in Figure 10 are now similar to but seem still to be slightly worse than those in Figure 5.

Figures 5 and 9–12 show that the characteristic neighbourhood recovered in parallel by thresholding the partial energies produces visually better results. The analytical sequential search behaves in this case almost as the empirical one if the larger neighbourhood is chosen. Although the sequential search for the top chi-square distance gives more appropriate interaction structures, these latter are still less efficient than the structures obtained in parallel. The simulation with the 16 analytically chosen clique families in Figure 11

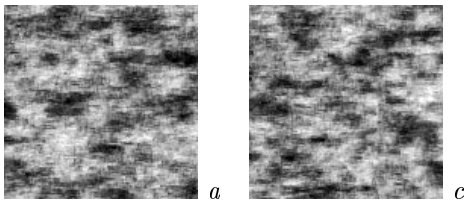

Figure 11: Texture D29: CSA-simulation with the 4 (a) and 15 (b) clique families found by the analytical sequential choice of the top relative Gibbs energy.

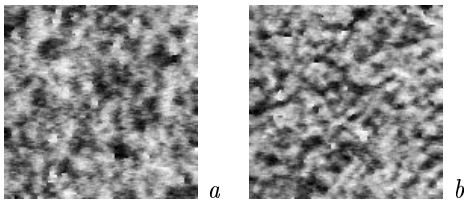

Figure 12: Texture D29: GLC-simulation with the 6 (a) and 16 (b) clique families found by the analytical sequential choice of the top relative chi-square distance.

is similar to the simulation with the 8-12 empirically found ones in Figure 10, and both simulations rank below the samples in Figure 5.

One possible reason of the ineffective sequential search is that the Gibbs energies do not properly manifest the assumed statistical relations between the GLCHs so that the detection of primary interactions and exclusion of secondary ones using the relative energies of Eq. (8) is not justified. In this case the sequential search can only deteriorate the actual interaction structure. The relative chi-square distances detect more accurately the secondary interactions for the stochastic texture D29 although the better or at least the same simulation quality is obtained under the initial assumption that all the interactions are almost independent. Similar results hold for the stochastic texture D77 in Figure 13 but here the sequential search results in the characteristic neighbourhood of smaller size.

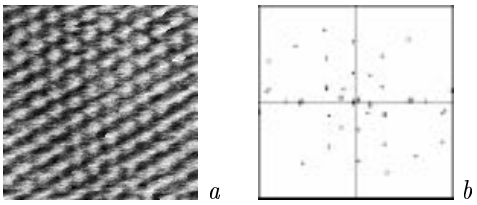

Figure 13: Texture D77: CSA-simulation (a) with the neighbourhood of 25 clique families (b) found by analytic sequential choice of the top relative Gibbs energy.

Figure 14 presents the D101 samples simulated once the interaction structure is estimated by the energy-based empirical sequential search. The training sample D101 is in Figure 2, *b*. Here, the final neighbourhoods of the 19–22 families both contain less clique families

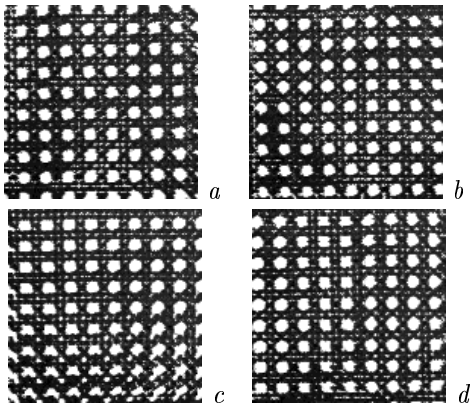

Figure 14: Texture D101: GLC-simulation with the 19 (a) – 22 (d) clique families found by the sequential empirical choice of the top relative Gibbs energy.

and represent better the fine repetitive details than the neighbourhood of the 63 families in Figure 8, *d*, found in parallel.

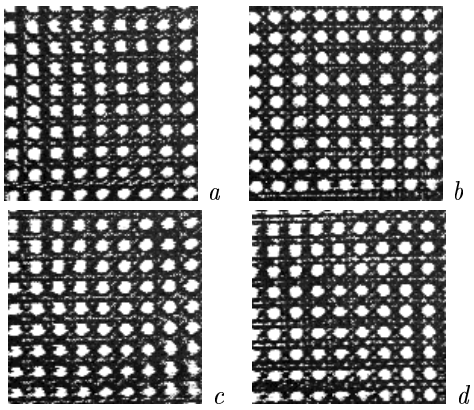

Figure 15: Texture D101: CSA-simulation with the 22 (a, c) and 63 (b, d) found by the analytical sequential choice of the top relative Gibbs energy and the top relative chi-square distance, respectively.

In this case the sequential choice forms a reduced characteristic neighbourhood of about 16–18 clique families describing the basic repetitive visual pattern. Then the additional 4–6 clique families describe the fine details of the texture. The visual quality of simulation does not steadily increase with the size of neighbourhood. As follows from Figure 14, *c*, the quality may even significantly degrade after adding the next clique family. But then usually the quality is restored and improved, once one or two more families are added. Unfortunately, it is still unclear how to relate the visual quality of simulation to certain quantitative features of a current pixel neighbourhood at each iteration t of the sequential search.

The analytical sequential search in Figure 15 creates the neighbourhoods of the 15–19 clique families describing roughly the basic repetitive pattern of the texture. The CSA-simulation with these nsmall eigh-

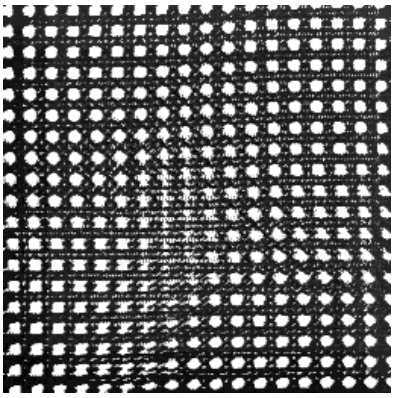

Figure 16: Texture D101: CSA-simulation with the 40 clique families found by the analytical sequential choice of the top relative Gibbs energy.

bourhoods produces the samples that are very similar to the samples in Figure 8, *c*-*d*, obtained with the neighbourhoods of the 39–63 families. But the search for the fine structure is less efficient so that two–three times larger neighbourhood of the analytically selected clique families is required to produce results similar to those for the empirically found neighbourhood.

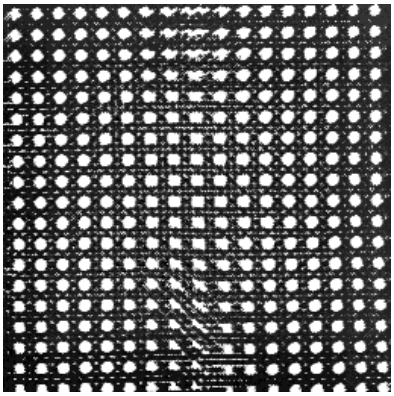

Figure 17: Texture D101: CSA-simulation with the 22 families found by the sequential empirical choice of the top relative Gibbs energy.

For comparison, the samples 256×256 in Figures 16 and 17 are simulated with the 40 and 22 clique families, respectively, chosen by the energy-based analytical and empirical search. The textures in Figure 16 and 15, *d*, represent fine repetitive details to the lesser extent than the samples in Figures 14 and 17 obtained by the empirical search. The analytical search based on the relative Gibbs energies works for the texture D101 better than the one based on the relative chi-square distances.

Figures 18 and 19 show the simulated samples of the texture D1. The characteristic neighbourhoods of the 13–16 and 37–40 clique families are obtained by the empirical sequential search of the top chi-square distance between the training and generated GLCHs. The training sample D1 is in Figure 2, *a*. As follows from Figures 7 and 18, the basic repetitive pattern is repli-

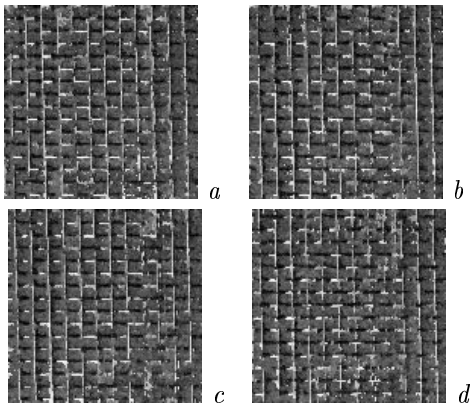

Figure 18: Texture D1: CSA-simulation with the 13 (a) – 16 (t) clique families found by the sequential empirical choice of the top relative chi-square distance.

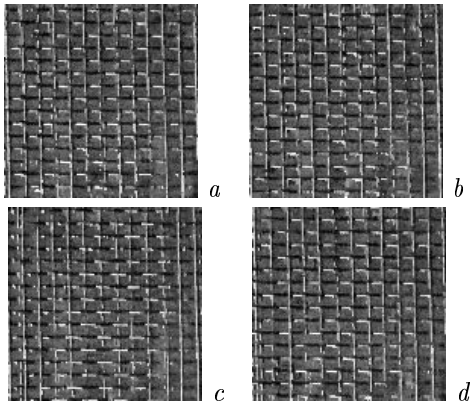

Figure 19: Texture D1: CSA-simulation with the 37 (a) – 40 (d) clique families found by the sequential empirical choice of the top relative chi-square distance.

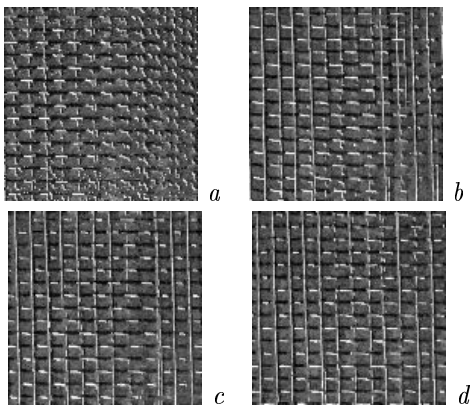

Figure 20: Texture D1: GLC-simulation with the 14 (a), 26 (b), 34 (c), and 40 (d) clique families found by the analytical sequential choice of the top relative chi-square distance.

cated by the neighbourhood that contains only 13–16 clique families. But then the 24–27 families have to be added to approximate with some degree of certainty the minor details of this texture. The visual quality of the samples simulated with the additional clique families in Figure 19 and 19 is considerably improved comparing to Figure 20.

Although the repetitive details of the regular texture D1 are reproduced less efficiently than those of the texture D101, the sequential search outperforms noticeably the parallel thresholding. The analytical scheme illustrated by Figure 20 presents here a reasonable alternative to the empirical one although the simulated samples seem to have a bit lesser visual quality than the samples in Figures 18 and 19.

6. Conclusions

These and other experiments in [3]-[5], as well as experiments in various colour and greyscale textures by the empirical sequential estimation of characteristic pixel neighbourhoods in [8], suggest that the Gibbs model of Eq. (2) can efficiently describe two classes of spatially homogeneous image textures, namely, the stochastic and regular textures. Clique families that form the characteristic interaction structures have different interdependences in each class.

The interaction structure of a stochastic texture consists of clique families with partial Gibbs energies (or chi-square distances to the IRF) over a particular threshold. All the families are assumed to be statistically independent so that the estimated neighbourhood cannot be reduced in size.

The structure of a regular texture contains both independent primary interactions and dependent secondary interactions produced by the primary ones. These interdependences permit us to reduce the size of a characteristic neighbourhood and recover more representative set of the primary interactions by the empirical or analytical sequential elimination of the secondary interactions. The sequential search produces efficient interaction structures only if our assumption about the independent primary GLCHs has a reasonable fit to the textures under consideration.

The empirical sequential scheme slightly outperforms the faster analytical one as concerning the fine repetitive patterns of regular textures. But the empirically and analytically found neighbourhoods that describe the basic, or rough repetitive patterns are very similar.

The sequential search for a characteristic pixel neighbourhood can exploit either the relative Gibbs energies or chi-square distances between the GLCHs for the training and simulated samples, but the chi-square distances give in some cases better description of a regular texture. At the same time, the sequential search may even deteriorate the interaction structure of a stochastic texture comparing to the parallel thresholding.

The empirical sequential search involves a substantial amount of computations. The alternative analytical scheme is much faster but reproduces only approximately the actual dependences between the primary and secondary interactions. Therefore, the analytical search has to produce larger characteristic neighbourhoods to approach, if possible at all, the quality of texture simulation after the empirical search.

Main drawback of the empirical sequential search is that the found characteristic neighbourhood depends on a particular chain of generated samples. Therefore the same training sample may produce different characteristic neighbourhoods, especially, as concerned the fine details of a repetitive pattern to be simulated. Also, all the sequential schemes as well as the parallel thresholding have no theoretically justified rules of choosing an adequate size of the pixel neighbourhood, and this size is selected on the experimental base.

Nonetheless, the estimated characteristic neighbourhoods and the corresponding GLCHs give a complete quantitative description of each texture with respect to the Gibbs random field model with multiple pairwise pixel interactions. Therefore, such a description should govern a choice of particular integral GLCH-based features for describing the stochastic or regular textures. In particular, the neighbourhoods $\mathbf{N_A}$ and corresponding GLCHs are efficient for a scale–orientation independent query–by–image texture retrieval [4]. In this case the similarity between a query image and the entries of an image data base is obtained first by matching only the neighbourhoods with exhausting possible scale and orientation transformations and then by using the chi-square distances between the normalised GLCHs.

References

[1] Brodatz, P., Textures: A Photographic Album for Artists an Designers, New York, Dover Publications, 1966.

[2] Chellappa, R., Jain, A. (Eds), Markov Random Fields: Theory and Application, Boston, Academic Press, 1993.

[3] Gimel'farb, G.L., Texture modeling by multiple pairwise pixel interactions, "IEEE Trans. Pattern Analysis Machine Intell.", 18, 1110–1114, 1996.

[4] Gimel'farb, G.L., Image Textures and Gibbs Random Fields, Dordrecht, Kluwer Academic, 1999.

[5] Gimel'farb, G.L., Basic and fine structure of pairwise interactions in Gibbs texture models, "Proc. Joint IAPR Int. Workshop on Syntactical and Structural Pattern Recognition and Statistical Pattern Recognition" (Alicante, Spain, 30 August - 1 Sept. 2000) (*in print*).

[6] Haralick, R.M., Statistical and structural approaches to textures, "Proc. IEEE", 67, 786–804, 1979.

[7] Haralick, R.M., Shanmugam, K., Dinstein, I., Textural features for image classification, "IEEE Trans. Systems, Man, and Cybern.", 3, 610–621, 1973.

[8] Zalesny, A.V., Analysis and synthesis of textures with pairwise signal interactions, Project 50542 (EC ACTS 074 "Vanguard"), Technical Report, Leuven, Katholieke Univ., 1999.